GEOMETRICALLY NONLINEAR STATIC ANALYSIS OF FUNCTIONALLY GRADED BEAMS SUBJECTED TO AXIAL CENTRIC FORCES

PHÂN TÍCH TĨNH PHI TUYẾN HÌNH HỌC CỦA DẦM CÓ ĐẶC TÍNH BIẾN THIÊN CHỊU LỰC DỌC TRỤC

Do Minh Duc, Le Cao Tuan

University of Science and Technology - The University of Danang; ducdhbk@gmail.com

Abstract - Since the neutral axis of a functionally graded (FG) beam does not coincide with the mid-plane, centrically applied forces *P* make the beam bend; on the other hand, the curvature deformation of the beam interacts with *P* causing additional moment, also known as the geometric nonlinear effect (*P*-δ effect). This paper investigates the geometric nonlinear effect of functionally graded beams subjected to axial static force. The material properties of the beam vary continuously in the thickness direction according to the power-law distributions. The governing equilibrium equations are established by using the principle of virtual work. The finite element method is employed to discretize the model and obtain a numerical approximation of the equilibrium equations. Numerical examples are carried out in Matlab programming language. The influences of geometric nonlinearity, boundary conditions, as well as different material property distributions on the behaviors of the beams are also analyzed and evaluated.

Key words - geometric nonlinearity; functionally graded beams; finite element method (FEM); stress; strain.

Tóm tắt - Do trục trung hòa của của dầm được chế tạo bằng vật liệu có đặc tính biến thiên (dầm FG) không trùng với trục hình học, lực tác dụng đúng tâm *P* sẽ làm cho dầm bị uốn; mặt khác, độ võng của trục dầm tương tác với *P* gây ra thêm mômen thứ cấp, mà còn được gọi là hiệu ứng phi tuyến hình học (hiệu ứng *P*-δ). Báo cáo này nghiên cứu hiệu ứng phi tuyến hình học của dầm có đặc tính biến thiên chịu tải trọng tĩnh dọc trục. Đặc tính của vật liệu giả thiết thay đổi liên tục theo chiều cao dầm theo quy luật hàm lũy thừa. Hệ phương trình cân bằng của dầm được thiết lập theo nguyên lý công khả dĩ. Phương pháp phần tử hữu hạn được sự dụng để rời rạc và tìm nghiệm xấp xỉ của hệ. Các ví dụ số được thực hiện với sự trợ giúp của phần mềm Matlab. Ảnh hưởng của tính phi tuyến hình học, các điều kiện liên kết ở biên cũng như hệ số phân bố vật liệu đến ứng xử của dầm được phân tích và đánh giá.

Từ khóa - phi tuyến hình học; dầm FG; phương pháp phần tử hữu hạn; ứng suất; biến dạng.

1. Introduction

Functionally graded materials (FGMs) are the next class composite materials whose material properties vary continuously from one surface to another. This is achieved by gradually varying the volume fraction of the constituent materials. FGMs are usually made from a mixture of metals and ceramics or combination of different metals to take advantage of each material's properties. Therefore, FGMs eliminate the stress concentration found in laminated composites and have good characteristics: high stiffness, thermal resistance, high strength-to-weight ratio, long fatigue life, corrosion resistance,… FGMs were first invented in Japan in 1984 by Sendai Group. This new kind material is widely used in different applications, such as reactor vessels, fusion energy devices, biomedical sectors, aircrafts, space vehicles, defense industries and other engineering structures, etc. [6]. With the wide application of FG structures, understanding their behaviors under external load acting is important.

During the last decades, analyses of FG structures have received much attention from the scientific community as reflected by increasing number of publications devoted to that. So far, there have been huge reports on static, buckling, and vibration analyses of these structures in the literature.

FG beams are used in aerospace, automotive industry, machine element, and other engineering structures. In addition, the applications of FG beams have broadly been spread in nano-electromechanical systems, thin films in the form of shape memory alloys, and atomic force microscopes to achieve high sensitivity and desired performance, Alshorbagy [3]. Some recent studies about static behaviors of FG beams [7-12], which are the closest researches to the study in this report, were fully reviewed in Ref. [4]. Hence, the contents and the solutions of these studies will not be given details here.

Since the material properties of an FG beam vary through the thickness direction, the neutral axis of such beam does not coincide with the mid-plane. Therefore, axially applied forces *P* make the beam bend. This problem is different from homogeneous beams, and it was well-investigated in the previous paper by Do et al. [5]. Moreover, the curvature deformation of the beam interacts with *P* causing additional moments, also known as the geometric nonlinear effect (*P*-δ effect). For FG beams, this complicated problem has not been studied and there is a need for serious examinations.

With the aim of extending from the previous work for the linear analysis in [5], this paper investigates the geometric nonlinear effect of FG beams subjected to axial static force. The material properties of the beam vary continuously in the thickness direction according to the power-law distributions. The governing equilibrium equations are established by using the principle of virtual work. The FEM is employed to discretize the model and obtain a numerical approximation of the equilibrium equations. Numerical examples are carried out in Matlab programming language. Finally, the influences of geometric nonlinearity, boundary conditions, as well as different material property distributions on the behaviors of the beams are also analyzed and evaluated.

2. Theoretical formulation

Consider a straight uniform functionally graded beam of length *L*, width *b*, thickness *h*, with coordinate system (O*xyz*) having the origin O is shown in Fig. 1, where the *x*-axis coincides with the mid-plane; the *y*-axis in the width direction and the *z*-axis in the depth direction. The beam is subjected to axial centric forces at the two ends.

2.1. Material properties

In this study, it is assumed that the effective Young's modulus (*E*) of the beam varies continuously in the thickness direction (*z*-axis) according to power-law form.

According to the rule of mixture [6], the effective Young's modulus (*E*) can be expressed as:

$$E(z) = E_L V_L + E_U V_U \quad (1)$$

where E_L, E_U and V_L, V_U are the corresponding Young's modulus and the volume fractions of two materials that compose the beam.

V_U and V_L are related by following equation:

$$V_U + V_L = 1 \quad (2)$$

Assuming that the V_U is varied by power law distribution as follows [6]:

$$V_U = \left(\frac{z}{h} + \frac{1}{2}\right)^k \quad (3)$$

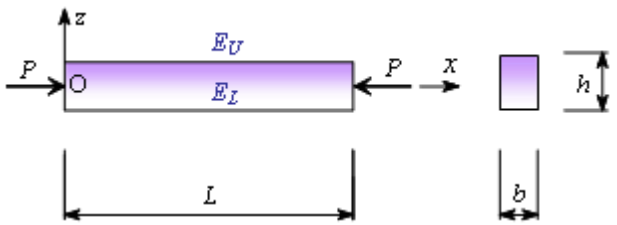

Figure 1. *A typical functionally graded beam with geometric parameters*

where *k* is the non-negative variable parameter (power-law exponent) which dictates the material variation profile through the thickness of the beam.

Therefore, substituting Eq. (3) into Eq. (2), then substituting all into Eq. (1), the effective Young's modulus (*E*) can be obtained as follows:

$$E(z) = (E_U - E_L)\left(\frac{z}{h} + \frac{1}{2}\right)^k + E_L \quad (4)$$

Some special cases drawn from Eq. (4) are:

- at $z = -h/2$, $E = E_L$ and at $z = h/2$, $E = E_U$
- $k = 0$, $E = E_U$ and the beam becomes homogeneous beam consisting of only *U* component.

2.2. The displacements and deformations on the beam:

Based on Euler-Bernoulli beam theory, the axial displacement, *u*, and the transverse displacement of any point of the beam, *w*, can be expressed in matrix form as below:

$$\{d\} = \begin{Bmatrix} u(x,z) \\ w(x,z) \end{Bmatrix} = \begin{bmatrix} 1 & 0 & -z \\ 0 & 1 & 0 \end{bmatrix} \{A_1\} \quad (5.b)$$

$$\{A_1\}^T = \left\{ u_o(x) \quad w_o(x) \quad \frac{\partial w_o(x)}{\partial x} \right\} \quad (5.b)$$

where u_o and w_o are the axial and the transverse displacement of any point on the mid-plane corresponding to displacement *u* and *w*, respectively.

The normal strain in the *x*-direction, ε_x, through the Von-Karman type nonlinear strain–displacement relations of the beam at a distance *z* can be represented by Eq. (6):

$$\varepsilon_x = \underbrace{\{1 \quad -z\}\{A_2\}}_{\varepsilon_1} + \underbrace{\frac{1}{2}\{1 \quad 1\}\{A_3\}}_{\varepsilon_2} \quad (6.a)$$

where

$$\{A_2\}^T = \left\{ \frac{\partial u_o}{\partial x} \quad \frac{\partial^2 w_o}{\partial x^2} \right\}; \{A_3\}^T = \left\{ \left(\frac{\partial u_o(x)}{\partial x}\right)^2 \quad \left(\frac{\partial w_o(x)}{\partial x}\right)^2 \right\} \quad (6.b)$$

ε_1 and ε_2 are, respectively, the linear and the nonlinear strain.

2.3. The strain-stress relation

Assuming the material of FG beam obeys Hooke's law, the strain-stress relationship equation can be written as Eq. (7) below [2]:

$$\sigma_x = E.\varepsilon_x = E(z).\varepsilon_1 + E(z).\varepsilon_2 \quad (7)$$

where σ_x is the axial normal stress.

2.4. The static equilibrium equations

In this study, FEM is employed to mathematically model the mechanical behavior of the beam.

The beam is discretized into elements. For each element subjected to an axial centric force *P*, the internal virtual work done by a stress field σ_x on a virtual strain field ε_x is equal to:

$$\delta W_e^{\text{int}} = \int_{V_e} \{\sigma_x\}_e^T . \{\delta\varepsilon_x\}_e . dV \quad (8)$$

where V_e is the volume of the beam element.

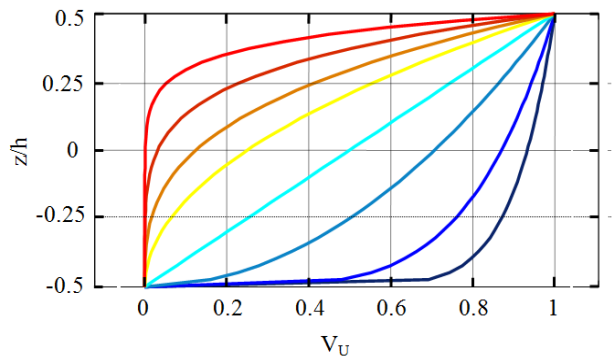

Figure 2. *Variation of the volume fraction V_u through the thickness of FG beam with respect to k*

By substituting Eq. (7) into Eq. (8) and then applying Hook' law to the linear strain ε_1 leads to Eq. (9)

$$\delta W_e^{\text{int}} = \int_{V_e} \{\varepsilon_1\}_e^T E(z) \{\delta\varepsilon_1\}_e \, dV + \int_{V_e} \{\sigma\}_e^T \{\delta\varepsilon_2\}_e \, dV \quad (9)$$

Next, substituting Eq. (6) into Eq. (9), we obtain:

$$\delta W_e^{\text{int}} = \int_0^l \{A_2\}^T [D]_E \{\delta A_2\} dx + \int_0^l \frac{1}{2} \begin{Bmatrix} P \\ P \end{Bmatrix}^T \{\delta A_3\} dx \quad (10)$$

where $[D]_E = b \int_{-h/2}^{h/2} \begin{bmatrix} E & -zE \\ -zE & z^2E \end{bmatrix} dz$ is the matrix of elastic coefficients, and l is the length of the element.

Approximate displacement of any point inside the element to the nodal displacements at the nodes through the shape function N_i [1]:

$$u_o^e = \Sigma N_i(x).q_e \ ; w_o^e = \Sigma N_i(x).q_e \quad (11)$$

where $\{q\}_e^T = \{u_i, w_i, \phi_i, u_j, w_j, \phi_j\}$: the element nodal displacement vector (tree degrees of freedom per node model is used)

Applying the principle of virtual work leads to the static equilibrium equation of a typical element which is described in the matrix form as below:

$$\left([K]_e + [K_G]_e\right)\{q\}_e = \{F\}_e \quad (12)$$

where $[K]_e, [K_G]_e, \{F\}_e$ are, respectively, the element elastic stiffness matrix, the element geometric stiffness matrix and the element nodal load vector.

Assembling all the element equations, we get the global equilibrium equations of the beam:

$$\left([K] + [K_G]\right)\{q\} = \{F\} \quad (13)$$

where $[K], [K_G]$ are the global stiffness matrices the and $\{F\}$ is the global load vector of the beam.

It is noted in this study that forces P, only applied at nodes, are inserted directly into the global load vector $\{F\}$ at the position corresponding with their degrees of freedom.

3. Numerical results and discussion

In this section, nonlinear static responses of the axially loaded FG beam as shown in Fig. 1 are investigated. Based on the presented theory above, a computational program is written in the Matlab programming language to solve the equilibrium equations and obtain the numerical results. Different boundary conditions, such as clamped-clamped (C-C), clamped-free (C-F), simply supported (S-S), clamped-hinged (C-H) end conditions, are considered. The width of the beam is taken as unity.

Functionally graded material of the beam, referred from Ref. [7], is composed of aluminum (Al) and alumina (Al_2O_3). Herein, the bottom surface of the beam is pure aluminum whose Young's modulus (E_L) is 70 GPa, whereas the top surface of the beam is pure alumina whose Young's modulus (E_U) is 380 GPa. In order to facilitate the presentation of results, dimensionless parameters are used as Eqs. (14) and (15) as follows:

$$\bar{w}(x) = 100 \frac{E_L h^2}{PL^2} w(x); \bar{\sigma}_x(x,z) = \frac{h}{P} \sigma_x(x,z) \quad (14)$$

$$P_{th} = \frac{\pi^2 E_L h^3}{12L^2}; \quad \eta = \frac{P}{P_{th}} \quad (15)$$

The analysis problems are: checking convergence and reliability of the presented theory and the written code; analyzing and discussing the effects of geometric nonlinearity, boundary conditions, as well as different material property distributions on the behaviors of the beams. Some important numerical results are calculated and given in tabular form, Tables 1-5, and in graphical form, Figs. 3-7.

3.1. Convergence and reliability

The convergence of the solution is determined through the number of elements used for the analysis. It can be seen in Table 1 that with a discretion of 100 elements -303 degrees of freedom, the accuracy of desired results is satisfactory. Therefore, next examples will correspond to the beam with those number elements.

In the special case of k = 0, the results in Tables 2-5 show that the values of transverse displacement ($\bar{w}$) are zero, and the values of normal stress ($\bar{\sigma}_x$) are equal to unity. This is exact because the FG beam becomes homogeneous beam; the applied force P becomes axial centric force and can not make the beam bend. In fact, the values of normal stress are approximate unity for the nonlinear analysis. It is due to the effect of the axial-

Table 1. *Values of mid-span deflection* $\bar{w}\left(\frac{L}{2}\right)$ *of (S-S) FG beams with respect to the element numbers (*η *= -1.0; L/h = 10)*

k	Number of elements							
	2	4	6	10	20	50	100	200
0	0	0	0	0	0	0	0	0
0.5	-4.4663	-4.4885	-4.4923	-4.4942	-4.4950	-4.4952	-4.4952	-4.4952
1	-10.0379	-10.1904	-10.2181	-10.2322	-10.2381	-10.2397	-10.2400	-10.2400
2	-19.6176	-20.2808	-20.4067	-20.4715	-20.4990	-20.5067	-20.5077	-20.5080
5	-28.0477	-29.2609	-29.4910	-29.6095	-29.6595	-29.6735	-29.6756	-29.6761
10	-28.0791	-29.0935	-29.2734	-29.3643	-29.4024	-29.4131	-29.4146	-29.4150
100	-24.8609	-26.2733	-26.3812	-26.4135	-26.4224	-26.4243	-26.4246	-26.4247

-nonlinear deformation-the first term in vector ε_2 in Eq. (6). The result also shows that this effect is very small; however, it is considered in all of the examples for the sake of generality in modeling.

3.2. Results and discussion

The results in Tables 2-5, Figs. 3-6 show the effect of geometric nonlinearity through the coefficient η. When η decreases, it reduces the geometric stiffness of the beam and leads to changes and increases in the value of the deflection compared to these of linear analysis. For example, the relative percentage increase of one case is (22.1625 – 11.0305)/11.0305 = 100.92% - for the non-dimensional mid-span deflection of the beam with k = 10, η = -0.8 and $L/h = 10$ (see the values in Table 2).

Table 2. *Variation of non-dimensional mid-span deflection* $\bar{w}\left(\frac{L}{2}\right)$ *of (S-S) FG beams with respect to* η *, k (L/ h =10)*

k	Linear analysis	Nonlinear analysis respect to η									
		-1	-0.8	-0.6	-0.4	-0.2	0.2	0.4	0.6	0.8	1
0	0	0	0	0	0	0	0	0	0	0	0
0.5	-3.1841	-4.4952	-4.1556	-3.8626	-3.6073	-3.3829	-3.0067	-2.8476	-2.7039	-2.5736	-2.4550
1	-6.3649	-10.2400	-9.1382	-8.2465	-7.5100	-6.8915	-5.9111	-5.5160	-5.1690	-4.8618	-4.5879
2	-10.5881	-20.5077	-17.3067	-14.9566	-13.1582	-11.7380	-9.6383	-8.8407	-8.1614	-7.5761	-7.0666
5	-12.7409	-29.6756	-23.5229	-19.4555	-16.5675	-14.4115	-11.4086	-10.3216	-9.4180	-8.6552	-8.0027
10	-11.0305	-29.4146	-22.1625	-17.7456	-14.7739	-12.6386	-9.7762	-8.7708	-7.9471	-7.2601	-6.6785
100	-2.7548	-26.4246	-9.8915	-6.0506	-4.3415	-3.3755	-2.3227	-2.0046	-1.7609	-1.5682	-1.4121

Table 3. *Variation of non-dimensional normal stresses of (S-S) FG beams* $\bar{\sigma}_x\left(\frac{L}{2},\frac{h}{2}\right)$ *with respect to* η *, k (L/ h =10)*

k	Linear analysis	Nonlinear analysis with respect to η									
		-1	-0.8	-0.6	-0.4	-0.2	0.2	0.4	0.6	0.8	1
0	1	1.0008	1.0006	1.0005	1.0003	1.0002	0.9998	0.9997	0.9995	0.9994	0.9992
0.5	0.7854	0.4943	0.5702	0.6354	0.6920	0.7416	0.8243	0.8591	0.8904	0.9186	0.9442
1	0.6242	-0.1586	0.0653	0.2459	0.3945	0.5188	0.7146	0.7929	0.8613	0.9216	0.9751
2	0.5785	-1.2550	-0.6593	-0.2238	0.1079	0.3686	0.7509	0.8948	1.0165	1.1207	1.2107
5	1.1959	-1.9182	-0.7785	-0.0287	0.5007	0.8935	1.4352	1.6290	1.7888	1.9224	2.0356
10	2.0481	-1.6450	-0.1773	0.7119	1.3066	1.7310	2.2933	2.4880	2.6460	2.7762	2.8853
100	4.6270	-1.4117	2.8266	3.8047	4.2355	4.4755	4.7302	4.8043	4.8595	4.9016	4.9345

Table 4. *Variation of non-dimensional normal stresses of (S-S) FG beams* $\bar{\sigma}_x\left(\frac{L}{2},0\right)$ *with respect to* η *, k (L/ h =10)*

k	Linear analysis	Nonlinear analysis with respect to η									
		-1	-0.8	-0.6	-0.4	-0.2	0.2	0.4	0.6	0.8	1
0	1	1.0008	1.0006	1.0005	1.0003	1.0002	0.9998	0.9997	0.9995	0.9994	0.9992
0.5	1.1239	1.1641	1.1537	1.1447	1.1369	1.1300	1.1185	1.1136	1.1091	1.1051	1.1014
1	1.1879	1.3275	1.2877	1.2556	1.2291	1.2068	1.1716	1.1575	1.1451	1.1341	1.1244
2	1.1170	1.4202	1.3221	1.2501	1.1952	1.1519	1.0882	1.0641	1.0436	1.0261	1.0108
5	0.8309	1.1163	1.0124	0.9438	0.8952	0.8589	0.8087	0.7906	0.7755	0.7629	0.7521
10	0.8220	1.0390	0.9534	0.9013	0.8662	0.8410	0.8072	0.7954	0.7856	0.7775	0.7706
100	0.9625	1.0142	0.9799	0.9714	0.9672	0.9645	0.9609	0.9596	0.9583	0.9572	0.9562

Table 5. *Variation of non-dimensional normal stresses of (S-S) FG beams* $\bar{\sigma}_x\left(\frac{L}{2},-\frac{h}{2}\right)$ *with respects to* η *, k (L/ h =10)*

k	Linear analysis	Nonlinear analysis with respect to η									
		-1	-0.8	-0.6	-0.4	-0.2	0.2	0.4	0.6	0.8	1
0	1	1.0008	1.0006	1.0005	1.0003	1.0002	0.9998	0.9997	0.9995	0.9994	0.9992
0.5	0.3994	0.4725	0.4535	0.4371	0.4229	0.4104	0.3896	0.3808	0.3729	0.3657	0.3592
1	0.6242	0.8552	0.7892	0.7360	0.6921	0.6553	0.5974	0.5742	0.5538	0.5359	0.5200

2	0.9536	1.5792	1.3763	1.2278	1.1145	1.0254	0.8945	0.8452	0.8033	0.7675	0.7364
5	1.2396	2.3145	1.9221	1.6634	1.4805	1.3445	1.1563	1.0888	1.0330	0.9862	0.9464
10	1.2597	2.3720	1.9313	1.6637	1.4843	1.3559	1.1851	1.1256	1.0771	1.0369	1.0031
100	1.0727	2.2885	1.4392	1.2419	1.1542	1.1046	1.0505	1.0341	1.0215	1.0115	1.0033

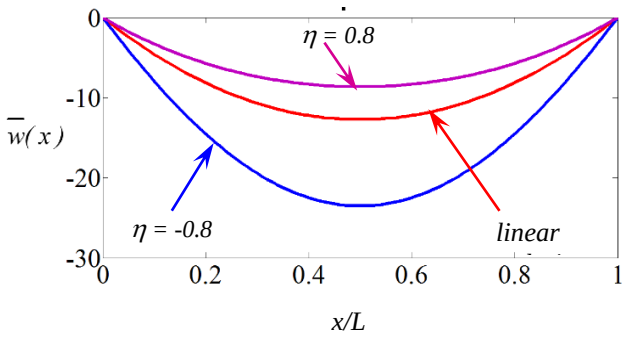

Figure 3. *Non-dimensional deflection of (S-S) FG beams along the length (k = 5, L/h = 10)*

Similarly, geometric nonlinearity also changes the stress distribution through the thickness of the beam. This change is quite complicated and depends on the distribution of material components. It can be seen from Tables 3-5 that when η decreases, the normal stress value (absolute value) tends to increase. This is due to the increase in additional bending moment caused by the second order effect (P-δ effect).

Effect of the distribution of material components in the FG beam, through the power-law exponent k, on the calculated values is illustrated in Tables 3- 4 and in Figs. 4-5. It is seen that:

-When k = 0, the FG beam becomes the homogeneous beam with full Al_2O_3 and no bending occurs at all. This phenomenon is deeply discussed in section 3.1

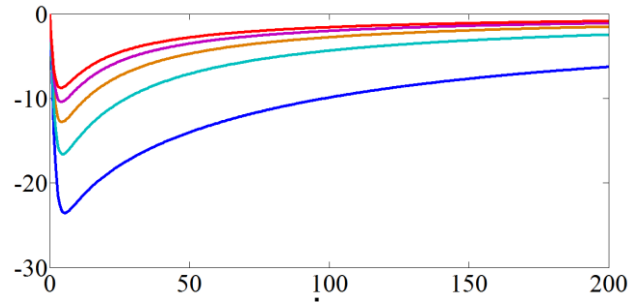

Figure 4. *Variation of non-dimensional mid-span deflection of (S-S) FG beams deflection* $\bar{w}\left(\frac{L}{2}\right)$ *with respect to k (L/h = 10)*

-When k gradually grows up, the deflection values increase. This is because of the reduced density of the Al_2O_3 constituent leads to the stiffness reduction of the beam and increase in the eccentricity of the neutral axis. It is also noteworthy that this eccentricity is reduced when k is greater than a finite value; thus, the deflection starts to decrease.

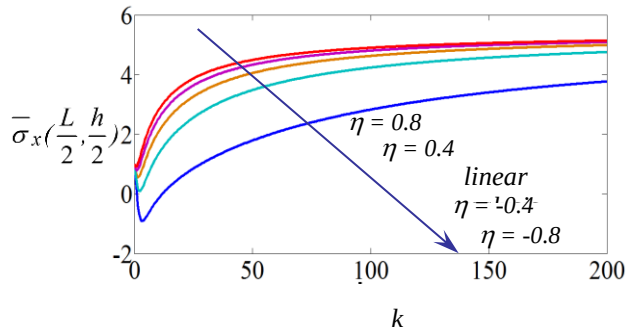

Figure 5. *Variation of non-dimensional normal stress of (S-S) FG beams* $\bar{\sigma}_x\left(\frac{L}{2},\frac{h}{2}\right)$ *with respect to k (L/h = 10)*

- As k approaches infinity ($k \to \infty$) the beam becomes full of Al; response of the beam is similar to the case of k = 0 which is investigated above. One could observe this phenomenon in Tables 3-5 and in Figs. 3-5 although power-law exponent k just reaches 100 and 200, respectively.

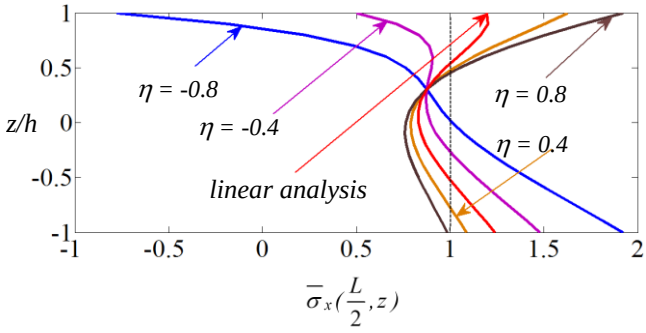

Figure 6. *Variation of non-dimensional normal stress* $\bar{\sigma}_x\left(\frac{L}{2},z\right)$ *through the thickness of (S-S) beams (L/h = 10, k = 5)*

The effect of different boundary conditions on the response of the beam is illustrated in Fig. 7. For (C-C) beam, the bending does not occur because the moment caused by the force P at the beam end is completely absorbed by the restraints; it is small for C-H beam compared to C-F and S-S beams. Especially, for the range ($-0.6 < \eta < -0.3$), it is in buckling region of the (C-F) beam, deflection value varies very largely, even approaches infinity. This problem is beyond the scope of the study and devoted for further investigation.

4. Conclusions

Geometric nonlinear effect on bending phenomenon of functionally graded beams subjected to a constant axial centric force is well-investigated and discussed. Euler-Bernoulli beam theory together Von-Karman type nonlinear strain-displacement relations and FEM are

employed to mathematically model the mechanical behavior of the beam. The material properties of the beam vary smoothly in the thickness direction according to the power-law distributions. Deflections, axial normal stresses are analyzed and discussed.

The numerical results show that geometric nonlinearity has significant effects on response of FG beams; different boundary conditions, power-law exponent *k* also change the stress distribution and deflection of the beams.

Despite being more complicated, geometric nonlinearity effect and nonlinear analysis give us a full and more accurate vision on responses of FG beams compared to linear analysis.

In the end, the present results can also be used as a benchmark for prospective research on bending of FG beams under axial loads.

REFERENCES

[1] Chu Quốc Thắng, *Phương pháp phần tử hữu hạn*, Nhà xuất bản khoa học kỹ thuật, Hà Nội, 1997.

[2] Đào Huy Bích, Nguyễn Đăng Bích, *Cơ học môi trường liên tục*, Nhà xuất bản xây dựng, Hà Nội, 2002.

[3] A-E. Alshorbagy, "Temperature effects on the vibration characteristics of a functionally graded thick beam", *Ain Shams Engineering Journal*, 4, 2013, pp.455–464

[4] Do Minh Duc, Le Khanh Toan, "Static analysis of functionally graded beams resting on elastic foundation using third-order shear deformation theory", *Review of ministry of construction*, 3, 2016, pp. 43-46.

[5] Do Minh Duc, Le Vu An, Le Khanh Toan, "Bending of functionally graded beams under axial force", *Conference on advanced technology in civil engineering towards sustainable development*, 2016, pp. 13-17.

[6] H.-S. Shen, *Functionally graded materials: nonlinear analysis of plates and shells*, Published by Taylor & Francis Group, LLC, 2009.

[7] H.-T. Thai, T.P. Vo, "Bending and free vibration of functionally graded beams using various higher-order shear deformation beam theories", *International Journal of Mechanical Sciences*, 62, 2012, pp. 57–66.

[8] J. Ying, C.F. Lu, W. Q. Chen, "Two-dimensional elasticity solutions for functionally graded beams resting on elastic foundations", *Composite Structures*, 84, 2008, pp. 209–219

[9] M. A. Benatta, I. Mechab, A. Tounsi, E.A. Adda Bedia, "Static analysis of functionally graded short beams including warping and shear deformation effects", *Computational Materials Science*, 44, 2008, pp. 765–773

[10] R. Kadoli, K. Akhtar, N. Ganesan, "Static analysis of functionally graded beams using higher order shear deformation theory", *Applied Mathematical Modelling* 32, 2008, pp. 2509–2525.

[11] T-K. Nguyen, TP. Vo, H-T. Thai, "Static and free vibration of axially loaded functionally graded beams based on the first-order shear deformation theory", *Composites: Part B*, 55, 2013, pp. 147–157.

[12] X-F. Li, B-L. Wang, J-C. Han, "A higher-order theory for static and dynamic analyses of functionally graded beams", *Arch Appl Mech*, 80, 2010, pp. 1197–1212.

(The Board of Editors received the paper on 05/09/2017, its review was completed on 25/10/2017)